Macromolecules

ARTICLE

pubs.acs.org/Macromolecules

Mechanically Tough Pluronic F127/Laponite Nanocomposite Hydrogels from Covalently and Physically Cross-Linked Networks

Chia-Jung Wu, Akhilesh K. Gaharwar, Burke K. Chan, and Gudrun Schmidt*

Department of Biomedical Engineering, Purdue University, 206 S. Martin Jischke Drive, West Lafayette, Indiana 47907-2032, United States

Supporting Information

ABSTRACT: Mechanical properties of polymer hydrogels are critical to their performance as tissue engineering scaffolds especially in load bearing tissues and wound sealants. In this study, we aim to synthesize mechanically tough nanocomposite hydrogels by photo-cross-linking PEO−PPO−PEO triblock copolymer diacrylates (Pluronic F127 diacrylate) in the presence of silicate nanoparticles, Laponite. The resulting hydrogels have high elongations and improved toughness when compared to their polymer hydrogel counterparts. Oscillatory shear and creep experiments suggest that the silicate nanoparticles physically interact with the covalently cross-linked polymer networks and impart viscoelasticity to the hydrogels. Imaging the structures of deformed nanocomposite hydrogels with cryo-scanning electron microscopy (cryo-SEM) leads us to believe that stretched hydrogels have finer network structures with smaller pore sizes when compared to the unstretched ones. The structural transitions observed in cryo-SEM and the viscoelastic properties measured suggest that noncovalent, physical interactions between Pluronic F127 and Laponite may contribute to rearrangements of network structures at high deformations. Overall, we expect the relationships between mechanical properties and network structures to provide valuable knowledge for the future design of high-performance hydrogels with use in a variety of biotechnological, biomedical, and pharmaceutical applications.

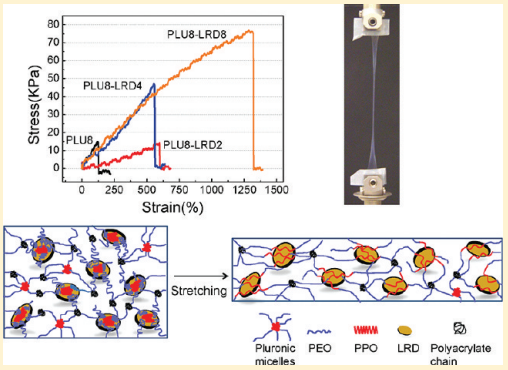

1. INTRODUCTION

Hydrogel properties such as swelling−deswelling,[1] stimuli-responsiveness,[2−4] liquid−gel transitions,[5,6] wet adhesiveness,[7,8] and shape memory effects[9] are promising for the development of a variety of biomedical and biotechnological applications ranging from wound dressings, surgical sealants, actuators, drug depots, and tissue engineering scaffolds. For example, hydrogels with liquid−gel transitions have great potential in tissue engineering and drug delivery because these hydrogels can be easily mixed with cells or drugs in the liquid state. After injection the hydrogels will solidify in situ to provide sustained delivery of treatments.

Poly(ethylene oxide)−poly(propylene oxide)−poly(ethylene oxide) (PEO_x−PPO_y−PEO_z), known as Pluronics, are thermosensitive triblock copolymers that display aqueous liquid−gel transitions important in injectable applications. These liquid−gel transitions are often characterized by a lower critical solution temperature (LCST) or a liquid crystalline phase transition.[6,10] Hydrogels based on PEO_{99}−PPO_{65}−PEO_{99} (Pluronic F127) have been increasingly used to deliver growth factors or cells to promote the regeneration of injured tissues.[11−14] Unfortunately, Pluronic F127 hydrogels are mechanically weak and dissolve in physiological environments very quickly,[15] which significantly limits their uses as load bearing tissue matrixes. In order to prevent dissolution and improve mechanical properties, the polymer can be end-functionalized with e.g. acrylate groups and then photopolymerized. The resulting covalently cross-linked hydrogels have improved mechanical properties when compared to conventional F127 hydrogel controls.[16,17] Although these covalently cross-linked hydrogels are resistant to dissolution, they are usually brittle and prone to fracture at low deformations.[18,19] Therefore, new approaches that can toughen polymer hydrogels will broaden their applications for use as tissue scaffolds that withstand extensive mechanical loadings.

Laponite, $(Na^{+}_{0.7}[(Mg_{5.5}Li_{0.3})Si_8O_{20}(OH)_4]^{-0.7})$, consists of synthetic silicate nanoparticles with an average diameter of 30 nm and a thickness of 1 nm. Laponite has been used to synthesize nanocomposite polymer hydrogels with unique mechanical properties.[20−25] For example, Haraguchi et al. used Laponite as a multifunctional cross-linker to synthesize poly(*N*-isopropylacrylamide) (PNIPAM)-based nanocomposite hydrogels (NC hydrogels). These materials show surprising extensibility with improved toughness when compared to hydrogels that were cross-linked by small molecules such as N,N' -methylenebisacrylamide.[20,21] In another study Wang et al. used Laponite and dendritic polymers to synthesize physically cross-linked and moldable hydrogels that can adhere to each other.[23] Loizou et al. cross-linked high molecular weight poly(ethylene oxide) with Laponite RD to prepare viscoelastic hydrogels (PEO-LRD hydrogels) with shear thinning

Received: March 11, 2011
Revised: August 5, 2011
Published: September 19, 2011

properties.[26,27] Other papers report on nanocomposites where Laponite was added to Pluronic F127 solutions to prepare hydrogels with temperature-dependent sol−gel transitions[28,29] and photogelling properties.[30]

Most recently, Fukasawa et al. reported on the development of nanocomposite hydrogels by incorporating Laponite nanoparticles into four-arm poly(ethylene glycol) hydrogels (tetra-PEG hydrogels).[25] Synthesis within a well-designed buffer system and careful sample preparation allowed for generating tetra-PEG nanocomposite hydrogels with improved tensile moduli, tensile strength, and elongation at break. However, these mechanical properties could only be obtained when the concentration of Laponite was relatively low (0.02 M or 1.6 wt %). When the concentration of Laponite was increased to more than 1.6 wt %, both ultimate strength and tensile moduli dropped significantly.[25]

These studies suggest that mechanical properties of hydrogels are system specific, and optimal hydrogel formulations depend on many parameters, among them the polymer chemistry, the type of cross-linking (covalent versus noncovalent = physical), and the degree of Laponite exfoliation. For example, literature indicates that Pluronic polymers are a better choice for preparing well-exfoliated Laponite dispersion than PEG.[31,32] When Pluronic type copolymers and Laponite are mixed in water, Laponite exfoliates and steric hindrance around Laponite nanoparticles often leads to the formation of low viscous, one-phase dispersions.[28,33] These dispersions may include high concentrations of Laponite which can be used to formulate nanocomposite hydrogels with a wide spectrum of mechanical properties tailored to specific applications.[22]

In this work, we report on the synthesis of photo-cross-linked nanocomposite hydrogels with elastomeric properties that allow extensive stretching up to 1300%. Photopolymerization have been used to prepare nanocomposite hydrogels in a time and space controlled manner,[34] which is useful to various applications such as tissue engineering, microfabrication, and drug delivery, etc. Here we photo-cross-link Pluronic F127 diacrylate solutions in the presence of Laponite RD. The resulting nanocomposite hydrogels have unique tensile properties with high elongations at break and are more viscoelastic than the polymer hydrogel counterparts. To investigate the relationships between microstructures and mechanical properties, the networks of the deformed nanocomposite hydrogels were imaged using cryo-SEM. Overall, the results obtained from this study are expected to further our fundamental understanding of how hydrogels can be toughened by silicate nanoparticles. If the mechanical properties of our hydrogels can be further developed to simulate specific biological tissue, then tissue engineering matrices for load bearing tissues can be generated.

2. EXPERIMENTAL SECTION

Materials. Pluronic F127 (PEO_{99}−PPO_{65}−PEO_{99}) was purchased from Sigma-Aldrich. Laponite RD (LRD), a synthetic hectorite with a thickness of ca. 1 nm and a diameter of ca. 30 nm, was received from Southern Clay Products Inc. The photoinitiator 2-hydroxy-1-(4-(hydroxyethoxy)phenyl)-2-methyl-1-propanone, Irgacure 2959 (I2959), was a kind gift from Ciba Specialty Chemicals. Dichloromethane and diethyl ether were purchased from Mallinckrodt Baker. Triethylamine was obtained from EMD Chemicals Inc., and acryloyl chloride was obtained from Alfa Aesar. All chemicals were used as received without further processing.

Synthesis of Pluronic F127 Diacrylate (PluDA). PluDA was synthesized according to procedures reported in the literature.[16] Briefly, 10 g of Pluronic F127 was dissolved in 100 mL of dichloromethane in a three-neck flask flushed with dry nitrogen gas at room temperature. The hydroxyl groups of Pluronic F127 were acrylated by adding 5-fold molar excess triethylamine and acryloyl chloride sequentially into the flask. The mixture was then stirred for 24 h under nitrogen gas and afterward filtrated to remove any precipitates. The product Pluronic F127 diacrylate (PluDA) was precipitated by adding above filtrate into excess chilled diethyl ether. The white precipitate was dried under vacuum for 1 day. The acrylation degree of PluDA was more than 90%, as determined by ^{1}H NMR on a Bruker ARX 400 Hz spectrometer and calculated by the ratio of acryl protons of PluDA (=CH_2, δ = 5.8−6.4) to methyl protons in poly(propylene oxide) groups (−CH_3, δ = 1.1). ^{1}H NMR (400 MHz, $CDCl_3$, δ): 5.8 (dd, 2H, CH_2=CH−COO−), 6.15 and 6.4 (dd, 2H, CH_2=CH−COO−), 1.1 (m, 195H, PPG methyl protons).

Preparation of Photo-Cross-Linked Nanocomposite Hydrogels. Precursor solutions of nanocomposite hydrogels were prepared by dissolving first PluDA and then LRD in deionized water containing 0.1% w/v initiator I2959. After adding LRD, the solution immediately becomes turbid. The turbid mixture was stirred for ca. 2 h to obtain a transparent solution. The fresh solution was used immediately to prepare photo-cross-linked nanocomposite hydrogels. 365 nm UV light (Black Ray B-100AP/R, UVP, LLC, CA) was used to covalently cross-link a precursor solution. The precursor solution was in a 0.9 mm thick silicone mold (dog-bone shaped or circular shaped) squeezed between two glass cover slips. The distance between UV lamp and precursor solution was 15 cm, and the photopolymerization took <10 min to complete. Since all hydrogels contained ca. 8% w/v PluDA and different amounts x of LRD, the samples were named as PLU8-LRDx.

Transmittance Measurement of Hydrogels. The transmittance of both precursor solutions and hydrogels was measured with a SpectraMax M5 microplate. PLU8 and PLU8-LRDx precursor solutions were photo-cross-linked for 3, 6, and 10 min, and their transmittance was measured at 650 nm.

Mechanical Testing of PLU8-LRDx Hydrogels. Tensile tests were performed on the as prepared PLU8-LRDx hydrogels using a TA ARES rheometer with torsion test geometry. The tested samples had a dog-bone shape. The crosshead speed used was 1 mm/s. The initial cross section of the center part of the dog-bone-shaped hydrogels (2.7 mm^2) was used for calculating the tensile stress. Tensile moduli were measured as the slope between 0 and 100% strain in the stress−strain curve. Toughness was calculated by measuring the area underneath the stress−strain curve of each sample. To determine the residual deformation of PLU8-LRDx hydrogels, the hydrogels were stretched from 2.5 to 10 cm. After stretching, the hydrogels were removed from the instrument and left on the top of a silicon sheet in a dish. The dish contained wet Kimwipes to prevent water evaporation. The length of hydrogels was measured at different times.

Swelling Ratio. As-prepared PLU8, PLU8-LRD2, and PLU8-LRD8 hydrogels were swollen in deionized water at 4 °C. The swelling ratio was calculated as the weight of the hydrogel at a specific time divided by its original weight. 4 °C was used to allow the hydrogels to fully swell because the Pluronic F127 polymer is more hydrophilic at low temperatures.

Cryo-Scanning Electron Microscopy (Cryo-SEM). Cryo-SEM was done on PLU8 controls, PLU8-LRD8, and stretched PLU8-LRD8 hydrogels in order to show differences in microstructures. For the stretched PLU8-LRD8 samples, the hydrogels were stretched uniaxially using a TA ARES rheometer 3 h before being imaged with cryo-SEM. The stretched hydrogels were "fixed" with tape and glue to maintain their elongated state. The stretched hydrogels and tape−glue constructs

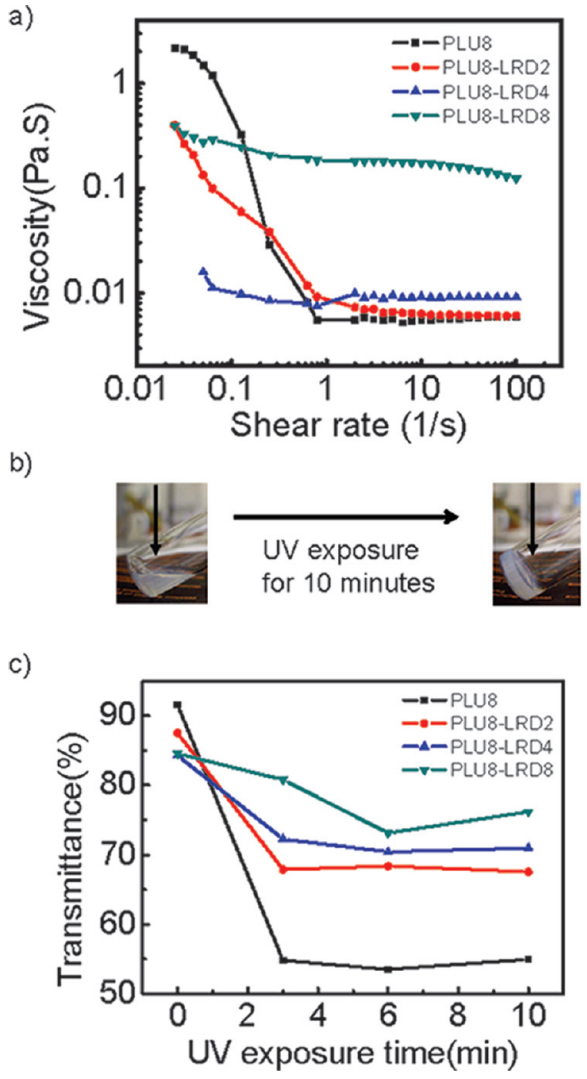

Figure 1. Viscosities of freshly prepared PLU8-LRD*x* precursor solutions before covalent cross-linking. (a) Viscosity measurements suggest that the precursor solutions are shear thinning at low shear rates. PLU8-LRD8 is less shear thinning due to interaction between PluDA and LRD. (b) Images show a low viscous precursor solution of PLU8-LRD8 and the cross-linked hydrogel that can sustain its own weight. (c) Transmittance measurements of PLU8-LRD*x* hydrogels show PLU8-LRD*x* hydrogels maintain high transparency during photopolymerization.

were then cryo-fractured by quickly plunging into liquid nitrogen. The frozen samples were then transferred to a Gatan Alto 2500 cryo unit (Warrendale, PA) and cut with a cold knife. The fractured and cut samples were sublimated at −90 °C for 8 min and then sputter-coated with platinum at −130 °C for 90 s. The coated samples were immediately observed and imaged with a FEI NOVA nano SEM (Hillsboro, OR) at −140 °C using 5 kV accelerating voltage.

Rheological Measurements. Stress sweep, frequency sweep, and creep experiments were used to investigate the viscoelastic properties of PLU8-LRD*x* hydrogels. All the rheological measurements were done on a TA AR2000 rheometer equipped with a Peltier plate for temperature control. A 20 mm parallel-plate geometry and a gap of 0.6 mm were used for all experiments which were done at 25 °C. A solvent trap prevented water evaporation during the measurements. All samples were tested for a linear viscoelastic region between 0.1 and 100 Pa, using stress sweep at a constant frequency of 1 Hz. Frequency sweep measurements were performed at a constant shear stress of 1 Pa. Creep experiments (constant stress) were done with an applied shear stress of 100 Pa for 10 min followed by 30 min of recovery. Data from creep experiments were evaluated by attempted fitting of the creep region with the Burger model.

$$J_c(t) = J_0 + J_1[1 - \exp(-t/\tau)] + t/\eta \quad (1)$$

$J_c(t)$ is the compliance of hydrogels measured by the instrument at time t, J_0 and J_1 are the instantaneous and retarded compliance corresponding to Maxwell and Kelvin−Voigt elements, respectively, τ is the retardation time, and η is the Newtonian viscosity.

3. RESULTS AND DISCUSSION

Characterization of Precursor Solutions and Photopolymerization. Figure 1a summarizes the viscosities of the PLU8-LRD*x* precursor dispersions/solutions and the PLU8 control as a function of shear rate. All as-prepared solutions are shear-thinning at low shear rates. At the higher shear rates viscosities do not change significantly. The PLU8-LRD8 dispersions are less shear thinning compared to the other compositions, suggesting more interactions between Laponite and PluDA molecules in water.

At low shear rates the PLU8-LRD*x* dispersions show lower viscosities than the PLU8 solutions. A similar phenomenon was observed by Boucenna et al., who found that the addition of Laponite nanoparticles decreased the elastic and loss moduli of concentrated Pluronic F127 solutions and increased their gelation temperature.[35] Both findings suggest that the addition of Laponite nanoparticles interferes with the assembly of Pluronic F127 micelles. This is probably happening because the preferential adsorption of Pluronic copolymers on the surfaces of Laponite nanoparticles (as suggested by Nelson et al.[33]) disturbs the formation of micelles and decreases the number of micelles in the bulk solution.

Most of the PLU8-LRD*x* precursor solutions/dispersions were transparent to the eye but some were slightly translucent, suggesting the presence of micrometer size aggregates that diffract visible light. The PLU8 solutions (controls) were transparent. The critical micelle concentration of Pluronic F127 in water at 25 °C is 4% w/v.[33,36] Therefore, there might be micelles present in the PLU8-LRD*x* solutions. However, the precursor solutions should only contain micelles and not form cubic liquid crystalline phase gels because these micellar cubic phases require polymer concentrations to be higher than 15% w/v.[10] PLU8-LRD*x* precursor solutions having LRD concentrations lower than ca. 8% w/v are low viscous, and those having LRD concentrations higher than 8% w/v are gel-like nonflowing dispersions. Here only low viscous precursor solutions having ≤8% w/v LRD were used. Because the PLU8-LRD*x* precursor dispersions become more viscous after storage (possibly due to electrostatic interactions between Laponite particles or cross-linking), all covalently cross-linked hydrogels were prepared from fresh prepared precursor solutions.

All PLU8-LRD*x* samples discussed here were photopolymerized with 0.1% w/v I2959 as initiators, and the final hydrogels contained 8% w/v PluDA and *x*% w/v of LRD. After UV-induced photopolymerization, both PLU8 and PLU8-LRD*x* solutions become hydrogels that can support their own weight (Figure 1b). The change in optical properties of PLU8 and PLU8-LRD*x* is shown in Figure 1c. The transmittance of the PLU8 hydrogel

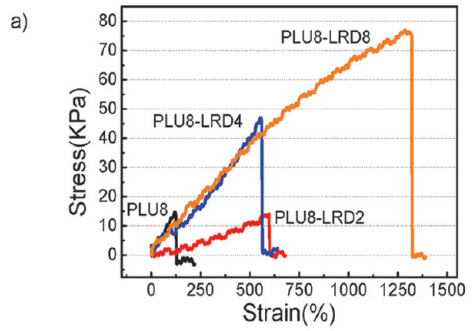

d)

Relaxation Time (hr)	Length (cm)		
	PLU8-LRD8	PLU8-LRD4	PLU8-LRD2
Before Stretching	2.5	2.5	2.5
0	3.60 ± 0.30	2.82 ± 0.10	2.42 ± 0.01
0.5	3.30 ± 0.15	2.62 ± 0.12	2.37 ± 0.01
1	3.18 ± 0.10	2.52 ± 0.05	2.35 ± 0.06
6	2.98 ± 0.13	2.47 ± 0.10	2.27 ± 0.01
24	2.83 ± 0.08	2.17 ± 0.05	2.05 ± 10.1

Figure 2. Tensile properties of PLU8-LRD*x* hydrogels. (a) Representative stress−strain curves of PLU8-LRD*x* hydrogels. (b) Image shows the stretched PLU8-LRD8 hydrogel during a tensile test. (c) Some residual deformation was observed when a PLU8-LRD8 hydrogel specimen was stretched to 700% strain and then removed from the instrument. Dashed rectangles marked on the image of sample after stretching show the hydrogel parts that were fixed to the grips (scale bar = 3 mm, hydrogel thickness = 0.9 mm). (d) Relaxation after deformation was recorded for PLU8-LRDx hydrogels immediately after stretching (time = 0) and after 0.5, 1, 6, and 24 h. The as prepared sample before stretching was 2.5 cm long.

control decreased significantly from 90% to 55% after UV exposure for 3 min. In contrast, the transmittance of PLU8-LRD*x* only dropped about 15% from 85% to 70%. Overall, the PLU8-LRD*x* hydrogels containing higher Laponite concentrations had higher transparency. These results suggest that addition of Laponite nanoparticles to the PLU hydrogel prevents structural heterogeneity that may occur during the polymerization of acrylate groups.

Tensile Properties of Photo-Cross-Linked Hydrogels Suggest High Elongations and Toughness. Figure 2a summarizes the mechanical properties of the photo-cross-linked hydrogels from tensile testing experiments. Figure 2b shows a hydrogel specimen during such a tensile test. Initial evaluation of results (Figure 2a) shows that the PLU8-LRDx hydrogels have higher elongations at break when compared to the PLU8 hydrogel controls. Among all PLU8-LRD*x* hydrogels, PLU8-LRD8 has the highest elongation at break (1300%) while maintaining a tensile strength around 76 kPa. However, after the tensile test is completed, the PLU8-LRD8 sample does not immediately relax to its original shape. The width of the sample remains somewhat narrower when compared to the original (Figure 2c). Thus, data suggest that some deformation remains after the tensile test is completed. We evaluated the residual deformation of PLU8-LRD*x* hydrogels and time-dependent relaxation after deformation. As part of these experiments the PLU8-LRD*x* hydrogels were stretched to 10 cm and then released from the grips. Their length after release from grips was measured with a ruler immediately and after 0.5, 1, 6, and 24 h (Figure 2d). The results show that the PLU8-LRD8 hydrogels after stretching relax from 3.6 cm slowly to 2.8 cm (measured after 24 h). The deformation that remained after 24 h implies that the polymer chains of PLU8-LRD8 hydrogels might rearrange during and after stretching.

In contrast to the toughness of PLU8-LRD8 hydrogels, PLU8 hydrogels that were tested as controls were more fragile with elongations at break being less than ca. 250% and tensile strengths less than 20 kPa. PLU8 hydrogels fractured easily at positions where the hydrogels were fixed to the grips, making it challenging to obtain reproducible measurements that prevent slippage during the tests.

When NC hydrogels are compared with our PLU8-LRD*x* hydrogels, Haraguchi's NC hydrogels tend to be fragile when high concentrations of covalent cross-linkers ($>3 \times 10^{-3}$ M) are used.[37] Our results however suggest that the PLU8-LRD*x* hydrogels maintain superior toughness and elongation at break even when synthesized using high amounts of PluDA covalent cross-linkers (6×10^{-3} M). A possible explanation for the brittleness of covalently cross-linked NC hydrogels is the formation of "microcomplex" structures where dense poly-NIPAM chains are attached to Laponite by covalent cross-linking.[37] Because of the presence of these structures, the transparency of covalently cross-linked NC hydrogels decreases significantly during hydrogel formation, and opaque hydrogels are produced. In contrast, PLU8-LRD*x* hydrogels contain ca. 6×10^{-3} M covalent cross-linkers (calculated by the molar concentration of PluDA) and the Laponite as noncovalent cross-linkers; thus, their elongation at break can be higher than 1000%. We observe only a slight decrease in transparency for our PLU8-LRD*x* hydrogels during photopolymerization (Figure 1c), while the resulting hydrogels are still transparent to eyes. The use of Pluronic diacrylate to fabricate hydrogels might prevent concentration fluctuations of small cross-linkers (like N,N'-methylenebisacrylamide), which very often results in opaque hydrogels with heterogeneous structures.[38]

The effects of Laponite on the overall tensile properties of PLU8-LRD*x* hydrogels show that an increase in Laponite concentration results in higher values for the elongation at break and improved tensile strength, while the moduli of PLU8-LRD*x* hydrogels remain lower than those of the PLU8 hydrogels. In our PLU8-LRD*x* hydrogels, both covalent cross-linking from polymerized acrylate groups and physical interactions between Laponite and polymer networks influence the tensile modulus. The moduli of PLU8-LRD*x* first decreased significantly when low concentration of Laponite was added and then increased with Laponite concentration. These results are in contrast to work on tetra-PEG NC hydrogels. The moduli of PLU8-LRD*x* decreased with LRD concentration at first and then increased again (Laponite: 2−8% w/v), while the moduli of tetra-PEG NC hydrogels increased first with Laponite concentration and then decreased (Laponite: >1.6 wt %).[25] In addition, the dependencies of tensile strength on Laponite concentration are also different between these two types of hydrogels. The tensile strength of PLU8-LRD*x*

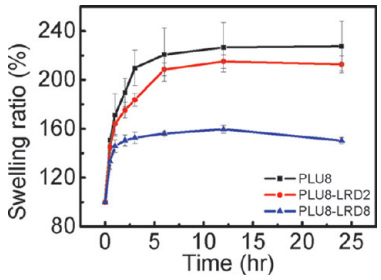

Figure 3. Swelling ratios of PLU8, PLU8-LRD2, and PLU8-LRD8 hydrogels at 4 °C. When the swelling ratios reach to plateau, PLU8-LRD2 and PLU8-LRD8 hydrogels both swell less than their polymer hydrogel counterpart.

Table 1. Statistics of Tensile Properties for PLU8-LRD*x* Hydrogels

sample name	maximal strength (kPa)[a]	elongation at break (%)[b]	toughness (kJ/m^3)[c]	tensile modulus (kPa)[d]
PLU8	22.2 ± 7.5	197 ± 83	24.24 ± 18.62	12.7 ± 1.2
PLU8-LRD2	18.5 ± 2.9	725 ± 120	55.52 ± 17.81	2.7 ± 0.2
PLU8-LRD4	48 ± 12.1	578 ± 37	128 ± 37.84	7.0 ± 2.2
PLU8-LRD8	76.7 ± 3.4	1308 ± 5	570.13 ± 18.92	9.8 ± 1.4

The mechanical properties in each category (column) are statistically different ($p < 0.05$) from each other except for the following pairs: [a] PLU8 and PLU8-LRD2, [b] PUL8-LRD2 and PLU8-LRD4, [c] PLU8 and PLU8-LRD2 and [d] PLU8 and PLU8-LRD8, and PLU8-LRD4 and PLU8-LRD8 (ANOVA with Tukey post-hoc analysis).

hydrogels increased with LRD concentration, while that of tetra-PEG NC hydrogels increased first and dropped significantly when Laponite concentration was higher than 1.6 wt %. The authors assumed that the high concentration of Laponite disturbed the formation of covalently cross-linked tetra-PEG networks. However, since the mechanical properties of PLU8-LRD*x* showed different trends when compared to the tetra-PEG-based hydrogels, we might assume that Laponite affects Pluronic and tetra-PEG networks differently.

A significant difference between the formulation of our PLU8-LRD*x* hydrogels and the tetra-PEG or PEG nanocomposite hydrogels mentioned previously is that the use of Pluronic F127 facilitates better exfoliation of Laponite nanoparticles, while the exfoliation of Laponite nanoparticles in tetra-PEG and PEG nanocomposite hydrogels seems to require a specific buffer system composed of pyrophosphate salts.[25] With optimized formulation the tetra-PEG/Laponite hydrogels have high elongations at break, maintain toughness and transparency, and have much improved mechanical properties compared to the tetra-PEG controls.[25] For comparison, a PEG−Laponite nanocomposite hydrogel reported by a different group showed tensile moduli only slightly higher than those of the PEG hydrogel controls.[24] As mentioned before, the adsorption of Pluronic F127 on the Laponite surfaces leads to steric hindrance between nanoparticles, which prevents aggregation. In contrast, the pyrophosphate within the tetra-PEG gels counterbalances the positive charge on the rim side of Laponite nanoparticles to prevent electrostatic interaction between nanoparticles. These different strategies to achieve exfoliation of nanoparticles might

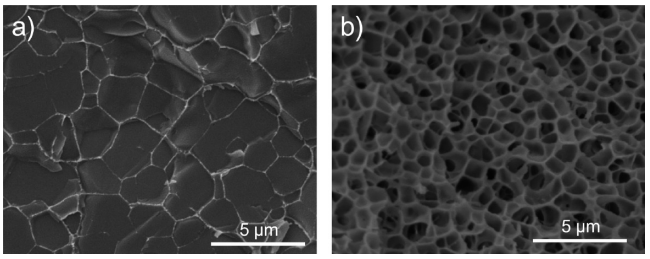

Figure 4. Cryo-SEM images of (a) PLU8 control and (b) PLU8-LRD8 hydrogels. The PLU8 hydrogel has an open network structure and pores with thin walls and large pore sizes. PLU8-LRD8 hydrogel images show a denser network structure composed of thicker pore walls and smaller pores. No aggregates or clusters were found when imaging on this length scale, suggesting LRD is well exfoliated in the hydrogel.

also influence the mechanical properties of the hydrogels, as PLU8-LRD*x* show their best mechanical properties at 8% w/v Laponite concentration while the tetra-PEG NC hydrogels at this concentration.

In order to examine whether the Laponite nanoparticles influence the polymerization of acrylate groups, which would result in increased swelling and decreased tensile moduli, the swelling ratios of PLU8, PLU8-LRD2, and PLU8-LRD8 were compared. As shown in Figure 3, after reaching the plateau, the swelling ratios of PLU8-LRD2 and PLU8-LRD8 hydrogels were lower than those of PLU8 hydrogels. These results suggest that photopolymerization in the presence of the Laponite nanoparticles does not enhance swelling but seems to provide additional cohesive forces to restrict hydrogel swelling. It is however possible that Laponite disturbs the formation of polymerized Pluronic F127 network as well, since the moduli of PLU8-LRD2 are much lower than that of PLU8. The increase in moduli from PLU8-LRD2 to PLU8-LRD8 (Table 1) suggests that Laponite might provide additional strengthening of the hydrogel network, probably due to the adsorption of polymer chains on the surface of Laponite.

Stretched Hydrogels Have Smaller Pore Sizes Due to Rearrangement of Physical Cross-Linkers. To better understand structure−property relationships, we compare the mechanical data obtained from selected PLU8-LRD*x* hydrogels with the cryo-SEM images from as prepared (relaxed) and stretched hydrogel networks. Cryogenic scanning electron microscopy (cryo-SEM) has often been used to image hydrated samples such as biological tissues or hydrogels. For example, Kim et al. used cryo-fixation techniques in combination with SEM to investigate how swelling affects the network of dextran−methacrylate hydrogels.[39] Matzelle et al. applied cryo-SEM techniques to investigate how the microstructure of PNIPAM hydrogels changes from their swollen state at room temperature to a collapsed state at 35 °C.[40] Similarly, Zhang et al. imaged the interpenetrating network structures of hydrogels composed of polymethacrylate and poly(*N*-isopropylacrylamide) under cryo-SEM conditions and found that the pore sizes of the hydrogels depend on temperature.[41] Therefore, cryo-SEM is a suitable technique that might provide morphological information related to the original hydrogel structure.

Figures 4 and 5 summarize results obtained from cryo-SEM that image PLU8-LRD*x* hydrogel films before mechanical deformation (unstretched) and in the deformed state (stretched). Only representative SEM images from fractured interior parts of hydrogels were shown, in order to avoid imaging artifacts from the hydrogel surface. At the examined length scale, no aggregates

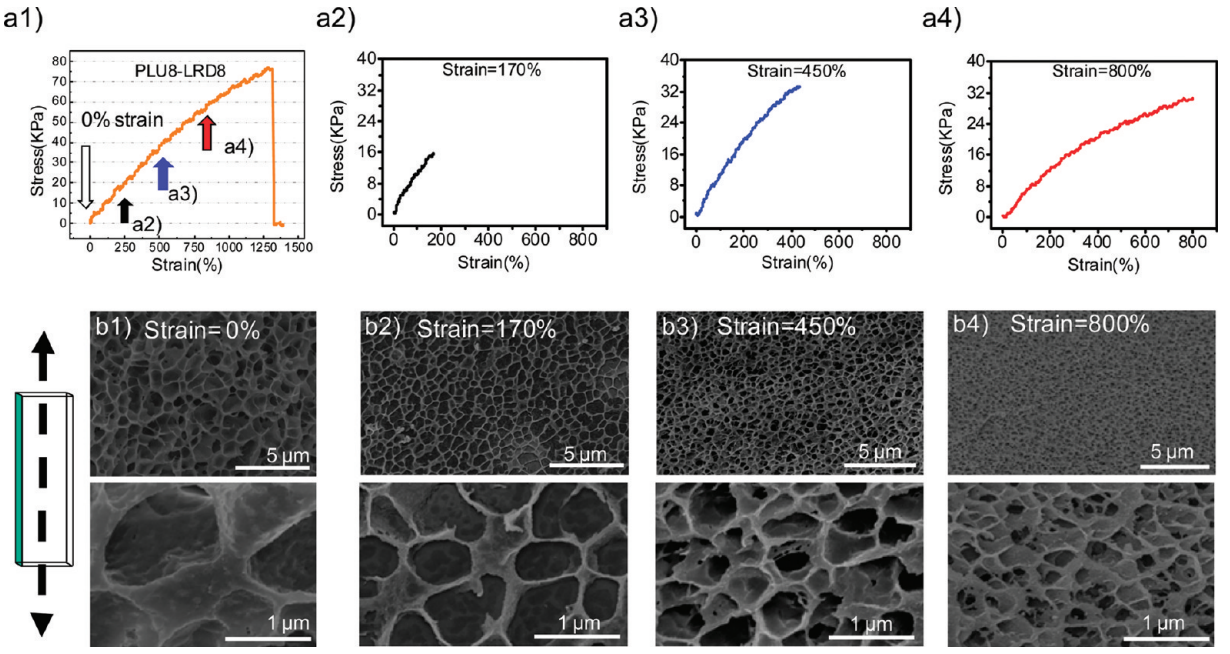

Figure 5. Mechanical testing data and cryo-SEM images of PLU8-LRD8 hydrogels at different strains. (a) Tensile tests for PLU8-LRD8 hydrogels at different strains. (b) Cryo-SEM images of PLU8-LRD8 hydrogels at rest and at different strains. Shaded area in cartoon on the left indicates plane of fractured hydrogel used for obtaining the cryo-SEM image. The imaged plane is parallel to the stretching direction. The overall results suggest that as the strain increases, the hydrogel network becomes finer and pore sizes become smaller.

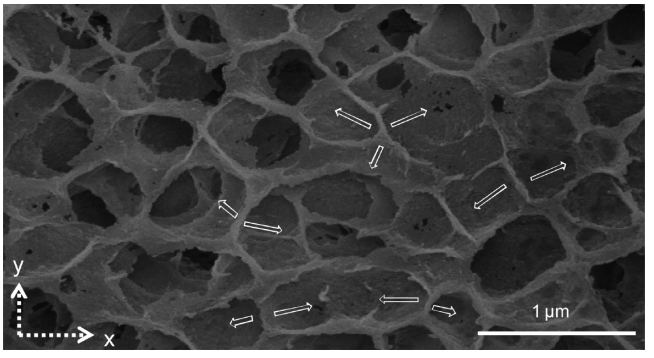

Figure 6. Cryo-SEM network features of a stretched PLU8-LRD8 hydrogel (~600% strain). The stretching direction is along the *x*-axis. No significant elongation in pores is observed.

were visible in any of the PLU8-LRD8 hydrogels, suggesting that Laponite was well-exfoliated in the precursor solutions. Figure 4 show the structures of "unstretched" PLU8 and PLU8-LRD8 hydrogels with differences in pore wall thickness and pore size. These differences are mainly a result of changes in composition. PLU8 hydrogels have thin pore walls and larger pores compared to the PLU8-LRD8 hydrogels that have thicker pore walls and smaller, uniform pore sizes of polyhedral shapes. A polyhedral morphology was previously observed in NC hydrogels.[42] The authors attributed the presence of polyhedral pores to the flexibility of polymer chains that deform during ice sublimation from frozen hydrogels, thus allowing the formation of the polyhedral morphology.[42] The pore sizes of PLU8-LRD8 hydrogels are significantly smaller than those seen in NC hydrogels reported previously,[42] possibly because of the higher concentration of Laponite nanoparticles used in PLU8-LRD8.

Table 2. Pore Sizes for PLU8-LRD8 with Different Strains

	strain (%)			
	0	170	450	800
mean (μm^2)	0.716 ± 0.588	0.511 ± 0.353	0.235 ± 0.104	0.152 ± 0.143
min	0.203	0.201	0.150	0.101
max	4.188	3.761	0.764	1.884
aspect ratio	1.8 ± 0.6	1.7 ± 0.5	1.8 ± 0.6	2.1 ± 0.8

In order to investigate how the hydrogel network responds to applied stresses, the PLU8-LRD8 hydrogels were stretched to 170%, 450%, and 800%, and then the hydrogels were imaged with cryo-SEM in the stretched state (Figures 5 and 6). The slopes of curves shown in Figure 5 a2, a3 and a4 are slightly different from each other because the tested samples are different. Surprisingly, no significantly elongated pores were found even after repeating these experiments several times, as the aspect ratios of pores do not significantly change with strain (Table 2). Instead, the pores observed seem to become smaller at the higher strains and the pore walls become thinner (Figure 6 and Table 2). As expected, a PEG hydrogel control showed elongated pores when stretched (Supporting Information Figure S1). Supported by our creep experimental data and results on residual sample deformation, we believe that one explanation for these astonishing results is that the physically cross-linked network between Laponite and polymer chains must be rearranging within the covalently cross-linked polymer network. Together with the stretching of polymer chains a large scale deformation of the hydrogel network is possible which is reflected in the high elongations observed. To fully understand this phenomenology

and to provide better proof of concept, more work needs to be done in the future.

Oscillatory Shear Experiments Suggest Large Viscoelastic Plateaus. When Laponite is added to a dilute PEO type polymer solution, viscoelastic dispersions form.[27] These dispersions show shear thinning behavior at large stresses and strains unless they are covalently cross-linked. Here, oscillatory shear experiments were used to determine viscoelastic properties of the covalently cross-linked PLU8-LRD*x* hydrogels. All samples were subjected to oscillatory shear stresses and frequency sweeps, and the materials responses were recorded. Results summarized in Figure 7a show that all the hydrogels have large viscoelastic regions within the range measured. As expected, G' of PLU8-LRD8 is much higher than G' of the other hydrogels. The higher G' of PLU8-LRD8 compared to the PLU8 controls was found to be in contrast to the results obtained from the tensile tests, where PLU8-LRD8 hydrogels show slightly lower tensile moduli than PLU8 hydrogels. One possible explanation for this contrast might be that the scales of deformation of these complex hydrogels are different when comparing rheological measurements and tensile tests. In rheological measurements, the deformation is very small, and Laponite might provide cohesive strength to resist the deformation. In tensile tests, however, the hydrogels are extensively deformed and Laponite nanoparticles might act as reversible cross-linkers that release stress. We also noticed that G'' increased with the LRD concentration, suggesting that LRD imparts viscous properties to the hydrogel network (Figure 7b).[43]

Frequency sweep measurements on PLU8-LRD*x* hydrogels were performed to better understand how LRD interacts with the polymer network. Results shown in Figure 7c indicate that the elastic moduli, G', of PLU8-LRD*x* increase with frequency and that G' is more frequency dependent when the LRD concentration is increasing. PLU8-LRD8 hydrogels have the highest G' and the highest change in G' with frequency when compared to the other samples. Slight increases in G' with frequency were found for PLU8-LRD4 and PLU8-LRD2 hydrogels. The G' of PLU8-LRD4 surpasses that of PLU8 when the frequency is higher than 5 Hz. Studies by Haraguchi et al. on NC hydrogels made from *N, N*-dimethylacrylamide and Laponite concluded that G' is frequency independent.[44] In a similar way, Abdurrahmanoglu et al. claimed that hydrogels made from acrylamide and Laponite have G' that are frequency independent although their published data shows that G' increased somewhat with frequency.[45] From these two studies, however, it is not clear if the observed small increases in G' with frequency (seen in their published data) is negligible and thus within the error bars.

Since frequency dependence of G' has been observed for other physically cross-linked hydrogels,[18,46] we conclude that G' of PLU8-LRDx hydrogels is frequency dependent because Laponite might physically interact with the polymer chains thus adding viscoelastic properties to the hydrogel. PLU8 hydrogel controls however do not show a frequency dependence of G' within the range measured, suggesting that the characteristics of the covalently cross-linked hydrogel network dominate.

Creep Experiments Confirm Viscoelastic Properties. The effect of LRD on the viscoelastic properties of PLU8-LRD*x* hydrogels is probably best observed in creep experiments. By fitting the creep curves of PLU8-LRD*x* hydrogels with Burger's model,[47] J_0, J_1, τ, and η can be obtained (Figure 8). Figure 8a highlights representative creep-recovery curves of PLU8-LRD*x* hydrogels. The shapes of the creep-recovery curves for PLU8-LRD*x*

a)

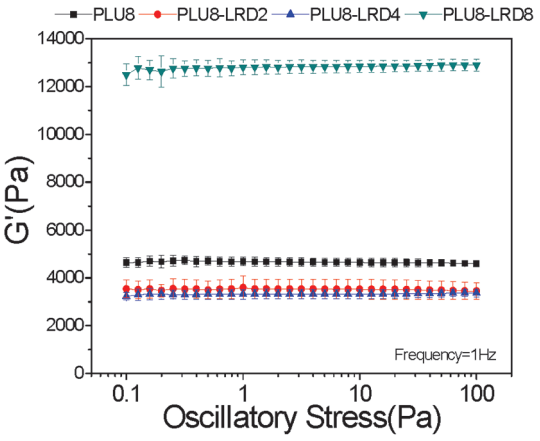

b)

Sample	G'(Pa)	G"(Pa)
PLU8	4671 ±189	122 ±22
PLU8-LRD2	3528 ±397	380 ±4
PLU8-LRD4	3313 ±200	617 ±33
PLU8-LRD8	12770 ±308	2370 ±81

c)

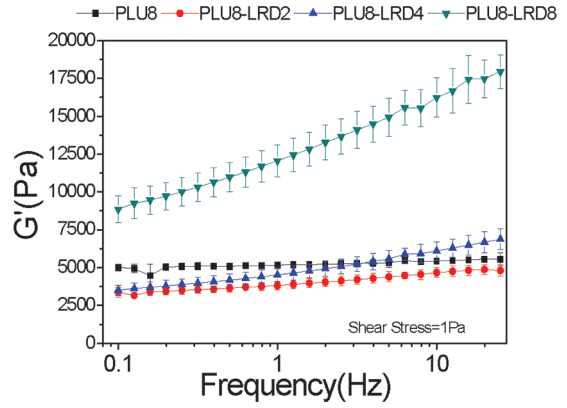

Figure 7. Oscillatory shear measurements on PLU8-LRD*x* hydrogels. (a) Stress sweep measurements show a linear viscoelastic region from 0.1 to 100 Pa. (b) Summary of G' and G'' at a shear stress of 1 Pa and a frequency of 1 Hz (data obtained from stress sweep experiments). (c) Frequency sweep measurements show frequency-dependent elastic moduli of PLU8-LRD*x* hydrogels. The dependency increases as the LRD contents increase. Notice that the elastic modulus of PLU8 does not significantly increase with frequency.

and the PLU8 control are different. The creep curve of the PLU8 hydrogel control shows a high initial compliance followed by a stable plateau region. After cessation of shear stress, PLU8 hydrogels show almost complete recovery. The creep curves and full recoveries measured suggest that PLU8 hydrogels have no significant structural rearrangements under examined conditions and thus behave similar to ideal cross-linked networks.[48,49] Data fitting was not performed on PLU8 hydrogels because no noticeable creep region was found. PLU8-LRD*x* hydrogels show time-dependent creep regions and only partial recovery after cessation of stress. From analyzing the J_0 and η data, one can follow the trends how the interactions between LRD and a covalently cross-linked polymer network affect elastic and viscous properties. When comparing these data to J_0 of PLU8 hydrogels, both PLU8-LRD2 and PLU8-LRD4 have a higher

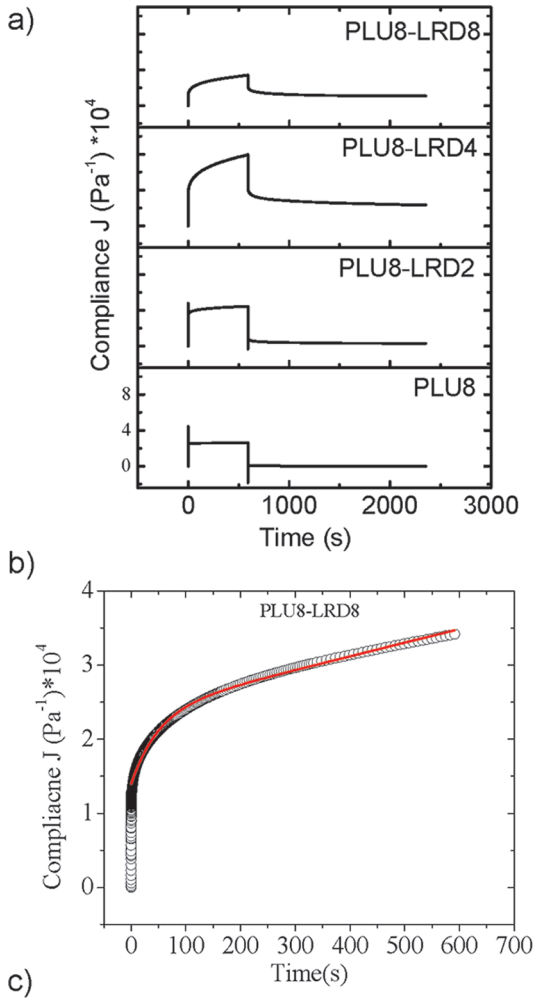

Sample Name	J_0(Pa^{-1})	J_1(Pa^{-1})	η(Pa·s)	τ(t)
PLU8-LRD2	3.5×10^{-4}	5.3×10^{-5}	1.4×10^{7}	29
PLU8-LRD4	3.9×10^{-4}	1.9×10^{-4}	2.8×10^{6}	49
PLU8-LRD8	1.4×10^{-4}	9.8×10^{-5}	5.4×10^{6}	49

Figure 8. (a) Representative creep and creep-recovery curves for PLU8-LRD*x* hydrogels. A shear stress of 100 Pa was applied to each hydrogel for 10 min to obtain the creep curves, and then stress was ceased to allow hydrogels recover. The *y* scale shown in (a) applies to each creep-recovery curve. All nanocomposite hydrogels show a creep region, while the PLU8 control does not. Except for the PLU8 control that fully recovers, all PLU8-LRD*x* hydrogels show only partial recovery after cessation of stress. (b) The creep region of PLU8-LRD8 shows attempted fitting with the Burger model. (c) Summary of data fitting results for PLU8-LRD2, PLU8-LRD4, and PLU8-LRD8 hydrogels.

compliance and only PLU8-LRD8 has a lower one. Because compliance is the inverse proportional to the modulus, this means that PLU8-LRD2 and PLU8-LRD4 hydrogels have lower elastic moduli and PLU8-LRD8 hydrogels have higher elastic moduli than the PLU8 control, which is in agreement with the data obtained from frequency and stress sweep experiments. On the other hand, η reflects the viscous behavior of PLU8-LRD*x* hydrogels, which suggests that physical cross-links are broken and rebuild when polymer chain movements are occurring under deformation. Thus, the PLU8 hydrogel control behaves more like an elastic material with short elongation at break and low toughness, while the PLU8-LRD*x* hydrogels are elastomeric-like but viscoelastic materials with long elongations at break and high toughness. The transition from an elastic hydrogel to a viscoelastic one shows the importance of polymer−Laponite interactions to the design of mechanical properties in PLU8-LRD*x* hydrogels.

Polymer−Laponite Interactions Leading to Mechanical Strength. Several studies suggest that both PPO and PEO absorb to the Laponite in water; however, the PPO has higher affinity to nanoparticle surfaces than the PEO.[33,50,51] PEO chains usually adsorb to the Laponite nanoparticles forming dense polymer layer on each nanoparticle face.[52] The interactions between the nanoparticles and the polymer chains lead to unique mechanical properties as observed in a variety of hydrogel systems. Low molecular weight polymers usually hinder aggregation of nanoparticles through steric hindrance. These effects either retard or prevent gelation of Laponite dispersions, thus decreasing the viscosity of the nanocomposite solutions, as we have observed for PLU8-LRD*x* precursor solutions. Higher molecular weight polymers below the threshold for complete saturation of nanoparticle surfaces build shake gels[53] which undergo shear thickening when subjected to vigorous shaking. PEO concentrations in excess of what is required to cover all Laponite surfaces lead to permanent hydrogels if the polymer chains are long enough to bridge between platelets. These physically cross-linked hydrogels are viscoelastic with gumlike consistency.[26,27]

The above-mentioned findings can be used to explain the mechanical properties of the PLU8-LRD*x* precursor solutions and hydrogels. In PLU8-LRD*x* precursor solutions, the PPO segments of $PEO_{99}-PPO_{65}-PEO_{99}$ preferentially adsorb to the surfaces of Laponite, and the PEO end chains cause steric hindrance which retards or prevents hydrogel formation. After photo-cross-linking the acrylate groups on the PEG ends form highly branched polymer networks. The polymerized molecules bridge adjacent Laponite nanoparticles which act as additional physical cross-linkers. Under low deformations, the polymerized network can be seen as near elastic. The polymer network should interconnect the physically attached Laponite nanoparticles, and viscoelastic properties should be expected at high deformations. These viscoelastic properties are suggested by our creep results, as all PLU8-LRD*x* hydrogels show increased strain/compliance with time. Furthermore, because the dynamic adsorption/desorption of polymer chains on the Laponite surfaces is sensitive to the applied forces,[27] the energy accumulated in PLU8-LRD*x* hydrogels should be more efficiently released by this dynamic process. The adsorption/desorption of polymer chains on Laponite surfaces is connected to the rearrangement of hydrogel networks, as suggested by our creep (Figure 8) and residual deformation data (Figure 2d). It is possible that the energy release caused during PLU8-LRD*x* hydrogel deformation is related to the hydrogels higher toughness (measured by tensile tests), especially when compared to the covalently cross-linked PLU8 control.

Our cryo-SEM results are surprising but could be explained by the unfolding and rearranging of polymer chains during deformation of the covalently and physically (noncovalently) cross-linked network (Figure 9). Because both PPO and PEO segments have affinity to the Laponite surfaces, the density of polymer around the Laponite surfaces will be high. Neutron

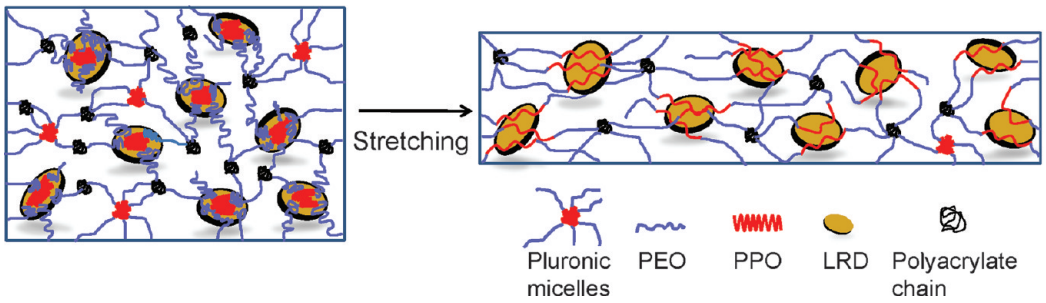

Figure 9. Schematic showing possible structural scenarios during network deformation in PLU8-LRD8 hydrogels. Covalent cross-linking of polymer chains leads to the formation of an elastic network, whereas physical cross-linking between Laponite and polymer chains induces viscoelastic properties. Before deformation, preferentially PPO polymer chains are attached to the LRD surfaces. During deformation, polymer chains are stretched, "unfolded" and rearranged. During this process the physical cross-linking may rearrange with attaching and detaching polymer chains. This rearrangement leads to finer hydrogel structures and smaller pore sizes at high elongations.

scattering studies on PEO−Laponite hydrogels already found that the PEO density around the Laponite surfaces was much higher than in the bulk solution.[52] The authors claimed that when shear was applied, the PEO chains will elongate and might be pulled away from the Laponite surfaces into the aqueous solution.[52] This theory might apply to our PLU8-LRD*x* hydrogels, leading us to believe that Pluronic F127 also forms a dense adsorption layer on the Laponite surfaces. When PLU8-LRD*x* hydrogels are subjected to uniaxial tensile testing, adsorbed polymer chains might be pulled away from the Laponite surfaces. It might be possible that the more strain the PLU8-LRD*x* hydrogels are subjected to, the more polymer chains are elongated and/or pulled from the surfaces of Laponite into the solution, leading to a "finer" structure with features such as thinner walls of pores and smaller pore sizes (Figure 5 and Table 2). Thus, the reversible movement of polymer chains between the surfaces of Laponite in an aqueous solution is responsible for properties such as higher elongations at break.

4. CONCLUSIONS

The structures and mechanical properties of both physically and covalently cross-linked nanocomposite hydrogels made from Pluronic F127 diacrylate and silicate nanoparticles (Laponite RD) were investigated. The nanocomposite precursor solutions were covalently cross-linked via photopolymerization. The resulting nanocomposite hydrogels have high elongations and improved toughness compared to their polymer hydrogel counterparts. Surprisingly, cryo-SEM images showed that stretched nanocomposite hydrogels have a finer network structure with smaller pore sizes compared to their structures before stretching. No significant elongation of pores was observed for the nanocomposites although the PEG control showed elongated pores. These structural results combined with the elastic and viscoelastic properties measured suggest that physical interactions between Pluronic F127 and Laponite may contribute to structural rearrangements when the nanocomposite hydrogels are subjected to high deformations. Thus, covalent cross-linking of polymer chains leads to the formation of an elastic network, whereas physical, noncovalent cross-linking between nanoparticles and polymer chains induces viscoelastic properties. Overall, we expect that the relationships between mechanical properties and network structure presented here will provide new knowledge for the future design of high-performance hydrogels.

■ ASSOCIATED CONTENT

Ⓢ Supporting Information. Cryo-SEM images of stretched hydrogels with elongated pores. This material is available free of charge via the Internet at http://pubs.acs.org.

■ AUTHOR INFORMATION

Corresponding Author

*Tel +1 765 496 1427; Fax +1 765 496 1912; e-mail gudrun@purdue.edu.

■ ACKNOWLEDGMENT

This research was supported in part by the Purdue Research Foundation and the Weldon School of Biomedical Engineering. We thank Debby Sherman for assistance with the cryo-SEM experiments.

■ REFERENCES

(1) Yoshida, R.; Uchida, K.; Kaneko, Y.; Sakai, K.; Kikuchi, A.; Sakurai, Y.; Okano, T. *Nature* **1995**, *374* (6519), 240–242.
(2) Qiu, Y.; Park, K. *Adv. Drug Delivery Rev.* **2001**, *53* (3), 321–339.
(3) Miyata, T.; Asami, N.; Uragami, T. *Nature* **1999**, *399* (6738), 766–769.
(4) Miyata, T.; Uragami, T.; Nakamae, K. *Adv. Drug Delivery Rev.* **2002**, *54* (1), 79–98.
(5) Jeong, B.; Bae, Y. H.; Kim, S. W. *J. Controlled Release* **2000**, *63* (1−2), 155–163.
(6) Wanka, G.; Hoffmann, H.; Ulbricht, W. *Macromolecules* **1994**, *27* (15), 4145–4159.
(7) Lee, B. P.; Dalsin, J. L.; Messersmith, P. B. *Biomacromolecules* **2002**, *3* (5), 1038–1047.
(8) Brubaker, C. E.; Kissler, H.; Wang, L.-J.; Kaufman, D. B.; Messersmith, P. B. *Biomaterials* **2010**, *31* (3), 420–427.
(9) Osada, Y.; Matsuda, A. *Nature* **1995**, *376* (6537), 219–219.
(10) Malmsten, M.; Lindman, B. *Macromolecules* **1992**, *25* (20), 5440–5445.
(11) Bromberg, L. E.; Ron, E. S. *Adv. Drug Delivery Rev.* **1998**, *31* (3), 197–221.
(12) Escobar-Chavez, J. J.; Lopez-Cervantes, M.; Naik, A.; Kalia, Y. N.; Quintanar-Guerrero, D.; Ganem-Quintanar, A. *J. Pharm. Pharm. Sci.* **2006**, *9* (3), 339–358.
(13) Dumortier, G.; Grossiord, J. L.; Agnely, F.; Chaumeil, J. C. *Pharm. Res.* **2006**, *23* (12), 2709–2728.
(14) Moore, T.; Croy, S.; Mallapragada, S.; Pandit, N. *J. Controlled Release* **2000**, *67* (2−3), 191–202.

(15) Lin, H. R.; Sung, K. C.; Vong, W. J. *Biomacromolecules* **2004**, *5* (6), 2358–2365.
(16) Lee, S. Y.; Tae, G. *J. Controlled Release* **2007**, *119* (3), 313–319.
(17) Missirlis, D.; Hubbell, J. A.; Tirelli, N. *Soft Matter* **2006**, *2* (12), 1067–1075.
(18) Kong, H. J.; Wong, E.; Mooney, D. J. *Macromolecules* **2003**, *36* (12), 4582–4588.
(19) Cha, C.; Kohmon, R. E.; Kong, H. *Adv. Funct. Mater.* **2009**, *19* (19), 3056–3062.
(20) Haraguchi, K.; Takehisa, T. *Adv. Mater.* **2002**, *14* (16), 1120–1124.
(21) Haraguchi, K.; Farnworth, R.; Ohbayashi, A.; Takehisa, T. *Macromolecules* **2003**, *36* (15), 5732–5741.
(22) Haraguchi, K.; Li, H. J. *Macromolecules* **2006**, *39* (5), 1898–1905.
(23) Wang, Q.; Mynar, J. L.; Yoshida, M.; Lee, E.; Lee, M.; Okuro, K.; Kinbara, K.; Aida, T. *Nature* **2010**, *463* (7279), 339–343.
(24) Chang, C.-W.; Spreeuwel, A. v.; Zhang, C.; Varghese, S. *Soft Matter* **2010**, DOI: 10.1039/c0sm00067a.
(25) Fukasawa, M.; Sakai, T.; Chung, U. I.; Haraguchi, K. *Macromolecules* **2010**, *43* (9), 4370–4378.
(26) Loizou, E.; Butler, P.; Porcar, L.; Kesselman, E.; Talmon, Y.; Dundigalla, A.; Schmidt, G. *Macromolecules* **2005**, *38* (6), 2047–2049.
(27) Loizou, E.; Butler, P.; Porcar, L.; Schmidt, G. *Macromolecules* **2006**, *39* (4), 1614–1619.
(28) Sun, K. S.; Raghavan, S. R. *Langmuir* **2010**, *26* (11), 8015–8020.
(29) Wu, C. J.; Schmidt, G. *Macromol. Rapid Commun.* **2009**, *30* (17), 1492–1497.
(30) Sun, K. S.; Kumar, R.; Falvey, D. E.; Raghavan, S. R. *J. Am. Chem. Soc.* **2009**, *131* (20), 7135–7141.
(31) De Lisi, R.; Gradzielski, M.; Lazzara, G.; Milioto, S.; Muratore, N.; Prevost, S. *J. Phys. Chem. B* **2008**, *112* (31), 9328–9336.
(32) De Lisi, R.; Lazzara, G.; Lombardo, R.; Milioto, S.; Muratore, N.; Liveri, M. L. T. *Phys. Chem. Chem. Phys.* **2005**, *7* (23), 3994–4001.
(33) Nelson, A.; Cosgrove, T. *Langmuir* **2005**, *21* (20), 9176–9182.
(34) Haraguchi, K.; Takada, T. *Macromolecules* **2010**, *43* (9), 4294–4299.
(35) Boucenna, I.; Royon, L.; Colinart, P.; Guedeau-Boudeville, M. A.; Mourchid, A. *Langmuir* **2011**, *26* (18), 14430–14436.
(36) Alexandridis, P.; Holzwarth, J. F.; Hatton, T. A. *Macromolecules* **1994**, *27* (9), 2414–2425.
(37) Haraguchi, K.; Song, L. Y. *Macromolecules* **2007**, *40* (15), 5526–5536.
(38) Shibayama, M. *Macromol. Chem. Phys.* **1998**, *199* (1), 1–30.
(39) Kim, S. H.; Chu, C. C. *J. Biomed. Mater. Res.* **2000**, *49* (4), 517–527.
(40) Matzelle, T. R.; Ivanov, D. A.; Landwehr, D.; Heinrich, L. A.; Herkt-Bruns, C.; Reichelt, R.; Kruse, N. *J. Phys. Chem. B* **2002**, *106* (11), 2861–2866.
(41) Zhang, J.; Peppas, N. A. *J. Biomater. Sci., Polym. Ed.* **2002**, *13* (5), 511–525.
(42) Haraguchi, K.; Matsuda, K. *Chem. Mater.* **2005**, *17* (5), 931–934.
(43) Okay, O.; Oppermann, W. *Macromolecules* **2007**, *40* (9), 3378–3387.
(44) Haraguchi, K. *Macromol. Symp.* **2007**, *256*, 120–130.
(45) Abdurrahmanoglu, S.; Okay, O. *J. Appl. Polym. Sci.* **2010**, *116* (4), 2328–2335.
(46) Jeong, K. J.; Panitch, A. *Biomacromolecules* **2009**, *10* (5), 1090–1099.
(47) Malkin, A. Y.; Isayev, A. I. *Rheology: Concepts, Methods & Applications*; ChemTec Publishing: Toronto, 2006.
(48) Rubinstein, M.; Colby, R. H. *Polymer Physics*; Oxford University Press: New York, 2003.
(49) Sperling, L. H. *Introduction to Physical Polymer Science*, 4th ed.; Wiley: New York, 2006.
(50) Nelson, A.; Cosgrove, T. *Langmuir* **2004**, *20* (24), 10382–10388.
(51) De Lisi, R.; Gradzielski, M.; Lazzara, G.; Milioto, S.; Muratore, N.; Prevost, S. *J. Phys. Chem. B* **2008**, *112* (31), 9328–36.
(52) Matsunaga, T.; Endo, H.; Takeda, M.; Shibayama, M. *Macromolecules* **2010**, *43* (11), 5075–5082.
(53) Zebrowski, J.; Prasad, V.; Zhang, W.; Walker, L. M.; Weitz, D. A. *Colloids Surf., A* **2003**, *213* (2−3), 189–197.